UDK 631.824: 621.7.015
Original scientific article/Izvirni znanstveni članek

ISSN 1580-2949
Mater. Tehnol.

SURFACE MODIFICATION OF MAGNESIUM FOR BIOMEDICAL APPLICATIONS: COMPARATIVE ANALYSIS OF PLASMA TREATMENT, LASER TEXTURING AND SANDBLASTING

POVRŠINSKA MODIFIKACIJA MAGNEZIJA ZA BIOMEDICINSKE APLIKACIJE: PRIMERJALNA ANALIZA PLAZEMSKE OBDELAVE, LASERSKEGA TEKSTURIRANJA IN PESKANJA

Marjetka Conradi*

Institute of metals and technology, Lepi pot 11, 1000 Ljubljana, Slovenia

Prejem rokopisa – received: 2025-04-18; sprejem za objavo – accepted for publication: 2025-04-28

doi:10.17222/mit.2025.1440

Magnesium and its alloys have emerged as promising materials for biomedical applications due to their light weight, mechanical compatibility with bone, biodegradability, and excellent biocompatibility. However, their rapid degradation in physiological environments remains a critical challenge. To address this, a range of surface-modification techniques have been explored to tailor the surface properties while preserving the bulk characteristics of magnesium. This paper provides an overview of surface-engineering methods aimed at enhancing the corrosion resistance, mechanical performance and bioactivity of magnesium. Three key surface-modification approaches are presented: plasma treatment, laser texturing and sandblasting. Plasma treatment resulted in the formation of a stable, protective oxide layer with significantly improved corrosion resistance and hydrophilicity. Laser texturing generated hierarchical microstructures yielding superhydrophobic surfaces with an enhanced hardness, though slightly reduced corrosion resistance. Sandblasting led to an increased surface roughness and mechanical stiffness, but also introduced microstructural defects that are detrimental to the corrosion stability. Overall, the study demonstrates how tailored surface modifications can effectively balance the mechanical integrity and degradation behavior of magnesium, paving the way for its optimized use in biomedical applications.

Keywords: magnesium, surface modification, biomaterial

Magnezij in njegove zlitine so se izkazali kot obetavni materiali za biomedicinske aplikacije zaradi svoje lahkosti, mehanske podobnosti s kostjo, biorazgradljivosti in odlične biokompatibilnosti. Kljub temu njihova hitra razgradnja v fizioloških okoljih ostaja ključni izziv. Za reševanje te težave so bile raziskane različne tehnike površinske modifikacije, ki omogočajo prilagajanje površinskih lastnosti ob hkratnem ohranjanju osnovnih lastnosti magnezija. Ta prispevek podaja pregled metod površinskega inženiringa, usmerjenih v izboljšanje korozijske odpornosti, mehanske zmogljivosti in bioaktivnosti magnezija. Predstavljeni so trije ključni pristopi površinske obdelave: plazemska obdelava, lasersko teksturiranje in peskanje. Plazemska obdelava je privedla do nastanka stabilne, zaščitne oksidne plasti z bistveno izboljšano korozijsko odpornostjo in hidrofilnostjo. Lasersko teksturiranje je ustvarilo hierarhične mikrostrukture, ki so omogočile nastanek superhidrofobnih površin z večjo trdoto, vendar nekoliko zmanjšano odpornostjo proti koroziji. Peskanje je povečalo hrapavost površine in mehansko togost, vendar je hkrati povzročilo mikrostrukturne napake, ki škodujejo stabilnosti proti koroziji. Primerjalna študija kaže, kako lahko ciljno usmerjene površinske modifikacije učinkovito uravnotežijo mehanske lastnosti in nadzorovanje razgradnje magnezija ter na ta način odpirajo možnost optimizirane uporabe magnezija v biomedicinskih aplikacijah.

Ključne besede: magnezij, površinska obdelava, biomaterial

1 INTRODUCTION

The light weight and superior biocompatibility, as well as the biodegradability, of magnesium and its alloys have gained a lot of attention in recent years.[1,2] Its density and elastic modulus closely resemble human bone, essential for minimizing stress shielding.[3–5] In addition, its unique non-toxic properties, make magnesium an excellent candidate for various biomedical materials.[6]

In general, implants are expected to successfully mimic the mechanical properties of human bones, to promote osteointegration, and degrade at a rate compatible with tissue growth, consequently leading to reduced healthcare expenses and repeated hospitalisations.[7–12] However, in a human-body-fluid environment, the presence of corrosive ions noticeably accelerates the degradation process of magnesium, leading to a rapid loss of mechanical integrity post-implantation.[13–15]

Therefore, various surface-modification techniques have been explored to control the degradation and enhance the bioactivity of Mg surfaces in the physiological environment.[16,17] There are, however, two main directions that lead to magnesium surface optimisation and have potential for enhancing corrosion resistance and biocompatibility, while preserving the bulk properties: coatings and surface microstructural modification.[18–20] In the past decade, a lot of work has been devoted to modification of the surface properties of magnesium, including ion implantation,[4,21] anodization,[22,23] plasma oxidation,[24]

*Corresponding author's e-mail:
marjetka.conradi@imt.si (Marjetka Conradi)

micro-arc oxidation,[13,25] laser texturing,[26–28] electro deposition, etc. These approaches aim to control the corrosion rates for magnesium-based implants. Overall, surface roughness is a critical factor influencing cell adhesion and osteointegration,[29,30] positioning surface roughening as a promising modification strategy that can enhance the bioactivity without altering the chemical composition of materials intended for biomedical applications.

In this paper, the latest progress on the surface modification of Mg surface is presented and the roles of various methods available for engineering the surface of Mg and its alloys are addressed. The influence of plasma surface treatment, laser texturing and sandblasting on the surface properties of Mg is presented and their influence on the surface properties, surface hardness and corrosion is compared.

2 MATERIALS AND METHODS

Materials. the magnesium rod (Goodfellow, 25 mm in diameter, 99.9 % purity, as drawn, E = 42.5 GPa) was cut into discs of thickness 2 mm. Prior to plasma treatment, laser texturing and sandblasting, the samples were diamond polished up to 1 μm.

Surface characterization. The surface morphology of the magnesium samples was evaluated with scanning electron microscopy FIB-SEM ZEISS Crossbeam 550 SEM. Optical 3D metrology system, model Alicona Infinite Focus (Alicona Imaging GmbH) and IF-Measure-Suite (Version 5.1) software were used to analyze the average surface roughness, Sa of the samples.

The X-ray photoelectron spectroscopy (XPS). XPS analyses were performed using Versa Probe 3 AD (Phi, USA) with a monochromatic Al-Kα X-ray source. The analyzed area was a spot with 200 μm diameter, and the analyzed depth was 3–5 nm. The survey spectra with three cycles were acquired at a pass energy of 224 eV and a step of 0.5 eV and high-resolution XPS spectra with at least 15 cycles were acquired at a pass energy of 69 eV and a step of 0.1 eV. During data processing, the carbon C 1s peak with the binding energy (BE) of 284.7 eV, characteristic for C–C bonds, was used to correct possible charging effects. The accuracy of the binding energies was estimated to be ± 0.2 eV. The measured spectra were processed with MultiPak 9.9.2 ULVAC-PHI software with Shirley background subtraction. High-resolution spectra for C 1s, O 1s and Mg 1s were analyzed.

Laser texturing. Surface texturing was performed with a LPKF nanosecond Nd-YAG laser with 1064-nm wavelength and an output power of 5 W. The system is equipped with a Scanlab SCANgine 14 processing head, which has an F theta-Ronar lens (F = 360 mm) and a double galvano configuration. SAMLight SCAPS v3.5.5 software was used for the programming of specific textures, i.e., dimples. The pulse length was 0.5 ms, the pulse frequency 500 Hz and the laser focus with a diameter of 30 μm was set on the Mg surface. The dimples with a diameter 50 μm and depth around 25 μm were arranged in a square formation with a center-to-center distance of 100 μm. Laser-texturing was performed in an argon atmosphere at room temperature without any post-treatment or post-polishing of the textured surface.

Sandblasting. Sandblasting (SB) was performed with a sandblasting device (Gostol TST d.d.), where the pressurized air in the device projected corundum particles (Al_2O_3, diameter between 212–250 μm, TESI Ltd.) at a 45° angle onto the magnesium surface. The distance between the nozzle and the sample surface was 20 cm and the air pressure was 6 bars. The sandblasting was carried out for 2 s, 5 s, 10 s and 30 s.

Wettability. The static water-contact angles at room temperature and ambient humidity were measured with a surface-energy-evaluation system (Advex Instruments s.r.o.).

Hardness.The nanoindentation measurements were conducted using the Hysitron TS 77 instrument from Bruker, employing a diamond Berkovich probe. A standard quasi-static load function was applied, featuring 5 s of loading, a 2-second holding period, and 5 s of unloading. The maximum load applied was 8000 μN. The nanoidentation hardness (H) and elastic modulus (E) were computed from the load-displacement curve, employing the Oliver and Pharr model.[31]

Potentiodynamic measurements. Potentiodynamic measurements were performed in simulated physiological Hank's solution (8 g/L NaCl, 0.40 g/L KCl, 0.35 g/L $NaHCO_3$, 0.25 g/L $NaH_2PO_4x2H_2O$, 0.06 g/L $Na_2HPO_4x2H_2O$, 0.19 g/L $CaCl_2x2H_2O$, 0.41 g/L $MgCl_2x6H_2O$, 0.06 g/L $MgSO_4x7H_2O$ and 1 g/L glucose, Merck chemicals) at room temperature and pH=7.8. The potentiodynamic curves were analyzed by using Bio-Logic SP-300 Model instrument and EC-Lab V11.27 software. The three-electrode electrochemical system was used with the test specimen as a working electrode, a saturated calomel electrode as a reference electrode and a platinum mesh as a counter electrode. The scan rate was 1 mV/s.

3 SURFACE MODIFICATION METHODS

3.1 Plasma surface treatment

Plasma can modify the surface properties of magnesium and its alloys in terms of surface chemistry, topography and wettability. With the direct plasma treatment, we can create a new, thicker, and pinhole-free oxide layer on the sample's surface which is surface protective and enables us to control both its corrosion resistance as well as its biocompatibility. If we treat the surface with two different kinds of plasma, i.e., H-mode (low pressure and high power) and E-mode plasma (high pressure and low power), we ensure that in the first step with hydrogen plasma the native magnesium oxide layer is completely removed, while the next step, treatment in oxygen plasma, leads to a controllable formation of a new oxide

Table 1: Plasma treatment parameters for modification of Mg surface with hydrogen and oxygen plasma

Plasma treatment	Gas	Pressure (Pa)	Power (W)	Time (s)	Gas	Pressure (Pa)	Power (W)	Time (s)
E mode H_2/O_2	H_2	25	600	10	O_2	40	200	300

layer. This allows us to manipulate the surface modification for specific applications. During the plasma surface modification, gas (oxygen/hydrogen) is introduced into the container and the pressure was adjusted according to the desired plasma treatment. The plasma treatment parameters are listed in **Table 1**.

3.2 Laser texturing

During laser texturing, rapid melting and cooling of the material significantly affects the microstructure of the magnesium surface and its surface properties. The morphology is defined with specific laser parameters such as power, frequency, speed and number of repetitions, resulting in various surface textures (i.e., lines, crosshatch, dimples). As shown in **Figure 1**. here, a square-like configuration of dimples with depth approximately 25 µm, diameter 50 µm, center-to-center distance 100 µm is presented.

3.3 Sandblasting

Sandblasting includes surface bombarding with abrasive Al_2O_3 (corundum) particles that are projected on to the surface at a specific angle. Surface modification is controlled by the distance between the nozzle and the sample surface, the air pressure and the time of the bombardment. Sandblasted surfaces show a significant change in the surface morphology with increased roughness due to the plastic deformation correlated to the impact of corundum particles. The degree of the plastic deformation is associated with the processing parameters. As shown in **Figure 2**, the variation of the time of sandblasting from 2 s, 5 s, 10 s and up to 30 s, led to an increase of the average surface roughness, *Sa,* with increasing time.

4 RESULTS AND DISCUSSION

4.1 XPS

XPS was used to determine the surface composition in the oxide layer of all the magnesium samples: DP, plasma treated, LT and SB. Three main elements were present on the surfaces: carbon, oxygen and magnesium. The chemical composition and ratios C/O and O/Mg are presented in **Table 3**. For all the surface-treated samples, we observe increase in oxygen and magnesium content in comparison to as-received diamond-polished sample. This confirms the pronounced formation of MgO as protection layer on all the samples.

Table 3: XPS evaluation: chemical composition in at% of as-received diamond polished, plasma treated surface, laser-textured and sandblasted Mg surfaces.

Sample	C	O	Mg	C/O	O/Mg
DP Mg	48.6	37.5	3.69	1.30	10.16
E mode H_2/O_2	21.30	49.90	7.24	0.43	6.89
LT	36.55	56.98	6.47	0.64	8.81
SB 5s	32.46	61.14	6.40	0.53	9.56

4.2 Surface hardness

The results of surface hardness measurements are listed in **Table 4** and show that the highest surface hardness, approximately 1.5 GPa, was observed in the la-

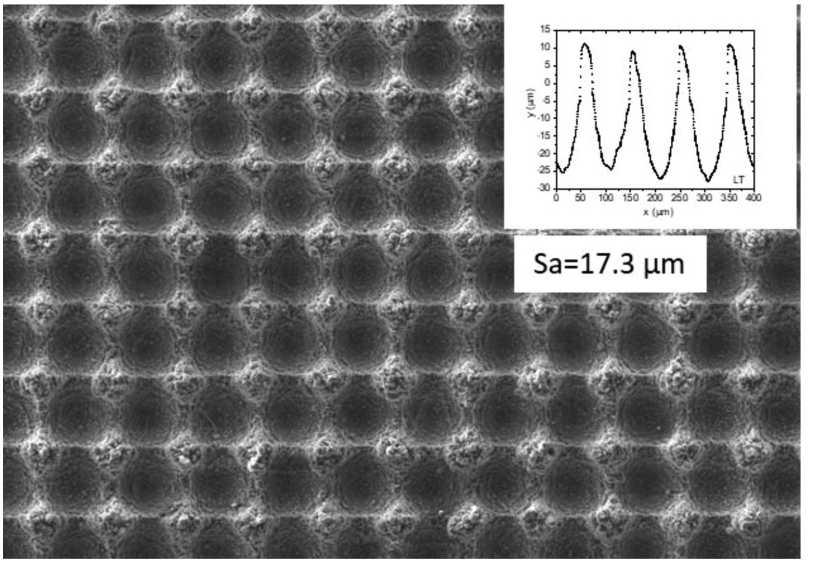

Figure 1: SEM image of laser-textured Mg surface. The inset shows average surface roughness

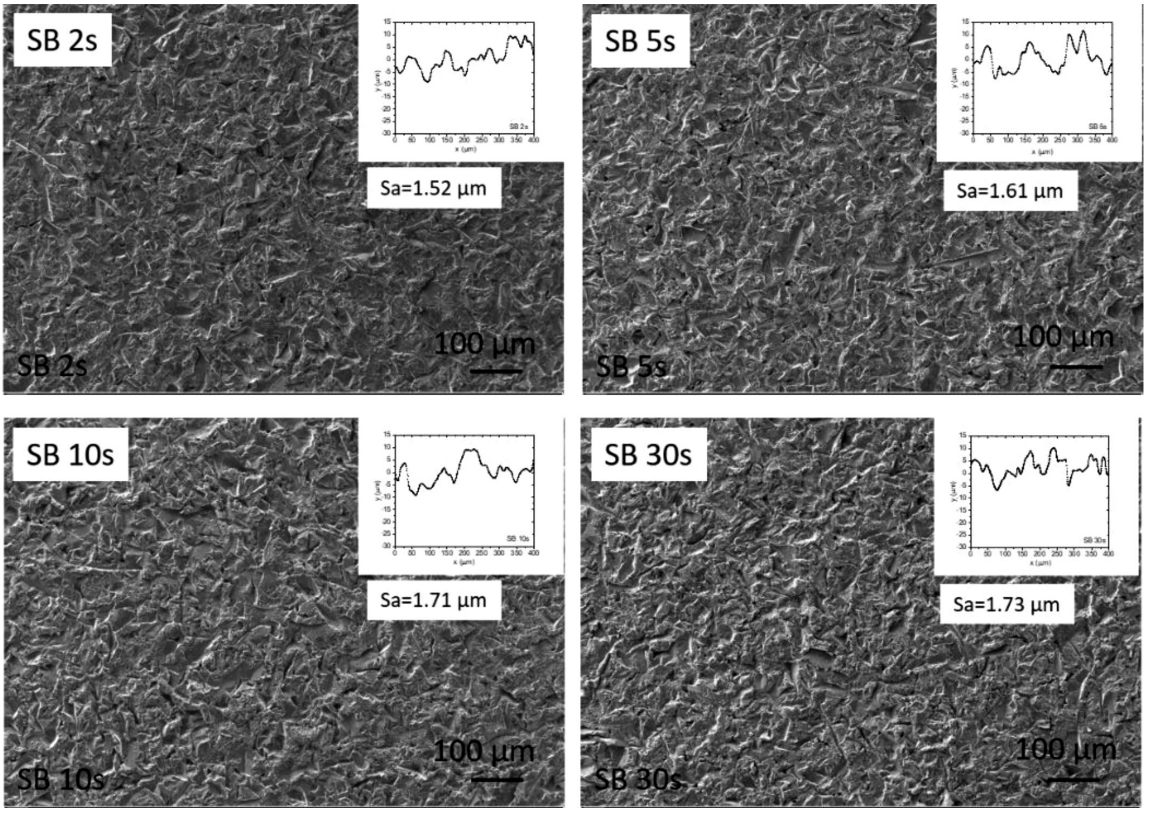

Figure 2: SEM images of sandblasted Mg surfaces with different times of sandblasting with corundum particles. The insets show the average surface roughness

ser-textured sample. This was followed by the samples sandblasted for 10 s and 30 s, which also showed an elevated hardness. In contrast, the plasma-treated, SB 2s and SB 5s samples exhibited hardness values similar to the reference DP surface, around 1 GPa. Surface hardness enhancement in magnesium is primarily associated with a grain-refinement caused by surface modification.[32–34] Laser texturing alters the microstructure through rapid heating and cooling, leading to recrystallization and localized surface oxidation. Similarly, the plastic deformation from sandblasting induces recrystallization and grain size reduction in the subsurface region.[26]

Table 4: Surface hardness (H) and Young's modulus (E) of as-received diamond polished, plasma treated surface, laser-textured and sandblasted Mg surfaces

Sample	H (Gpa)	E (Gpa)
DP	1	38 ± 2
E mode H_2/O_2	1	42 ± 2
LT	1.5	45 ± 3
SB 2s	1	45 ± 4
SB 5s	1	45 ± 3
SB 10s	1.2	60 ± 4
SB 30s	1.2	51 ± 4

A comparison of the Young's modulus (E) between surface-treated samples and the reference DP magnesium shows an overall increase in stiffness and resistance to deformation for all the treated surfaces. The highest modulus, approximately 60 GPa, was recorded for the SB 10s sample, followed by the SB 30s with E = 51 GPa. The LT, SB 2s, and SB 5s samples exhibited similar Young's modulus values, around 45 GPa. The lowest Young's modulus was measured for the plasma treated surface, around 42 GPa, which is still higher than that of the untreated DP surface, measured at around 38 GPa.

4.3 Wettability

The surface wettability was analysed by measuring five static water contact angles on the sample's surface. The average values of the contact angles are listed in **Table 5**. The diamond-polished surface, which serves as the reference, is moderately hydrophilic with a contact angle of 75°. With respect to contact-angle values, as listed in **Table 5**, two extreme surfaces are observed: plasma treated, which is strongly hydrophilic and laser-textured which is superhydrophobic. Strong hydrophilicity of plasma treated surface can be explained with XPS results, which indicate a decrease of the C content in comparison to all other Mg surfaces (**Table 3**). This is in agreement with the trend of the surface wettability being governed by the adsorption of organic matter from the atmosphere.[34,35] The superhydrophobic nature of laser-textured surface is, however, governed by the hierar-

chical surface structure, which is a consequence of micro/nano structuring effect reflected in increased surface roughness.

The sandblasted surfaces are moderately hydrophilic; however, their wettability is related to the time of sandblasting. SB 2s surface is neutrally wet with a contact angle slightly above 90°. As shown in **Table 5**, the contact angles decrease and the surfaces become more hydrophilic with the increasing time of sandblasting. This is also in correlation to the increased average surface roughness, suggesting that the sandblasted surfaces are in the Wenzel wetting regime, allowing us a controllable surface wettability according to the chosen sandblasting parameters.[35]

Table 5: Static water contact angles and average surface roughness.

Sample	θ (°)	Sa (μm)
DP Mg	75 ± 2	0.25 ± 0.02
E mode H_2/O_2	28 ± 1	0.28 ± 0.02
LT	>150 (superhydrophobic)	17.3 ± 1.2
SB 2s	94 ± 3	1.52 ± 0.14
SB 5s	77 ± 2	1.61 ± 0.15
SB 10s	68 ± 2	1.71 ± 0.16
SB 30s	60 ± 2	1.73 ± 0.16

4.4 Electrochemical evaluation

The corrosion behavior of DP, E mode H_2/O_2, LT, SB 2s, SB 5s, SB 10s and SB 30s magnesium samples in simulated physiological solution with electrochemical parameters, i.e., corrosion potential (E_{corr}), corrosion current density (i_{corr}) and corrosion rate (v_{corr}), is evaluated in **Table 6**. Overall, a significant decrease of i_{corr} and v_{corr} (0.2 mm/year) is observed for the plasma-treated surface E mode H_2/O_2. According to the trend in contact angles (**Table 5**), one would instinctively assume a decreased corrosion resistance for the plasma-treated samples compared to the untreated Mg. However, the increased corrosion stability of the plasma-treated Mg can be attributed to the increased oxygen content on the surface, as determined by XPS as well as the formation of a MgO component.[24]

On the other hand, significant surface roughness changes due to the surface modification of LF and SB samples can have a negative effect on the corrosion behaviour. In laser texturing, the recrystallization of magnesium occurs as a result of melting followed by rapid solidification. In contrast, sandblasting induces plastic deformation in the subsurface layer due to the high kinetic energy of the impacting particles, which also leads to the formation of voids and microcracks. Both surface treatments promote recrystallization, resulting in grain refinement and twin formation. While this enhances surface hardness, it simultaneously reduces corrosion resistance.[26] The lower corrosion resistance observed in both laser-textured (LT) and sandblasted (SB) samples can also be attributed to a reduced oxygen-to-magnesium (O/Mg) ratio on the surface (Table 3). However, the LT sample exhibits a less significant increase in corrosion rate, likely due to its superhydrophobic properties and high surface roughness.

Table 6: Electrochemical parameters of as-received diamond-polished, plasma treated surface, laser-textured and sandblasted Mg surfaces.

Sample	E_{corr} (V vs. SCE)	i_{corr} (μA/cm^2)	v_{corr} (mm/year)
DP Mg	–1.64 ± 0.03	35.4 ± 0.5	1.62 ± 0.05
E mode H_2/O_2	–1.63 ± 0.03	4.1 ± 0.1	0.18 ± 0.01
LT	–1.89 ± 0.04	63.7 ± 0.3	2.91 ± 0.01
SB 2s	–1.62 ± 0.03	334.7 ± 0.5	15.29 ± 0.03
SB 5s	–1.62 ± 0.03	293.8 ± 0.5	13.43 ± 0.03
SB 10s	–1.61 ± 0.03	382.5 ± 0.5	17.48 ± 0.04
SB 30s	–1.56 ± 0.02	373.5 ± 0.5	17.07 ± 0.04

5 SUMMARY AND OUTLOOK

In this study, the surface modification of magnesium via plasma treatment, laser texturing, and sandblasting was systematically investigated to evaluate their influence on the surface characteristics, hardness, wettability, and corrosion behavior in simulated physiological conditions. The plasma treatment was found to significantly improve the corrosion resistance and enhance the surface hydrophilicity due to the formation of a protective oxide layer with a high oxygen content. Laser texturing introduced hierarchical surface structures that imparted superhydrophobic properties and increased surface hardness, albeit at the cost of slightly elevated corrosion rates. Sandblasting effectively modified the surface morphology and improved the mechanical properties, with hardness increasing proportionally to treatment duration; however, this came with a considerable drop in corrosion resistance, primarily due to induced microstructural defects and reduced O/Mg ratios.

Overall, plasma treatment emerged as the most promising technique for biomedical applications where controlled degradation and biocompatibility are critical. Laser texturing offers advantages in applications where enhanced hardness and water repellency are desirable, while sandblasting can be used to tailor the roughness and mechanical behavior with careful control of the parameters. Future work should focus on combining surface modification methods (e.g., plasma treatment followed by laser texturing) to synergistically enhance both corrosion resistance and mechanical performance.

Acknowledgement

The author acknowledges the financial support from the Slovenian Research Agency (research core funding No. P2-0132 and L2-4445).

6 REFERENCES

[1] Gupta M, Wong WLE. Magnesium-based nanocomposites: Lightweight materials of the future. Mater Charact 2015;105:30–46. doi:10.1016/J.MATCHAR.2015.04.015

[2] Zhang S, Jiang J, Zou X, Liu N, Wang H, Yang L, et al. Progress of laser surface treatment on magnesium alloy. Front Chem 2022;10. doi:10.3389/fchem.2022.999630

[3] Schumacher SA, Toribio RE, Lakritz J, Bertone AL. Radio-Telemetric Assessment of Cardiac Variables and Locomotion With Experimentally Induced Hypermagnesemia in Horses Using Chronically Implanted Catheters. Front Vet Sci 2019;Volume 6-2019. doi:10.3389/fvets.2019.00414

[4] Zhang J, Zhang B, Zhang J, Lin W, Zhang S. Magnesium Promotes the Regeneration of the Peripheral Nerve. Front Cell Dev Biol 2021;Volume 9-2021. doi:10.3389/fcell.2021.717854

[5] Shang Z, Li D, Chen J, Wang M, Zhang B, Wang X, et al. The Role of Biodegradable Magnesium and Its Alloys in Anterior Cruciate Ligament Reconstruction: A Systematic Review and Meta-Analysis Based on Animal Studies. Front Bioeng Biotechnol 2021;Volume 9-2021. doi:10.3389/fbioe.2021.789498

[6] Zoroddu MA, Aaseth J, Crisponi G, Medici S, Peana M, Nurchi VM. The essential metals for humans: a brief overview. J Inorg Biochem 2019;195:120–9. doi:10.1016/J.JINORGBIO.2019.03.013

[7] Khan M, Osman K, Green G, Haddad FS. The epidemiology of failure in total knee arthroplasty. Bone Joint J 2016;98-B:105–12. doi:10.1302/0301-620X.98B1.36293

[8] Dauwe J, Walters G, Holzer LA, Vanhaecht K, Nijs S. Failure after proximal humeral fracture osteosynthesis: a one year analysis of hospital-related healthcare cost. Int Orthop 2020;44:1217–21. doi:10.1007/s00264-020-04577-y

[9] Herteleer M, De Jaegere A, Winckelmans T, Casteur H, Nijs S, Hoekstra H. Healthcare utilization and related cost of midshaft clavicle fracture treatment in Belgium. Eur J Trauma Emerg Surg 2021;47:1281–7. doi:10.1007/s00068-020-01307-2

[10] Xi W, Hegde V, Zoller SD, Park HY, Hart CM, Kondo T, et al. Point-of-care antimicrobial coating protects orthopaedic implants from bacterial challenge. Nat Commun 2021;12:5473. doi:10.1038/s41467-021-25383-z

[11] Virtanen S. Biodegradable Mg and Mg alloys: Corrosion and biocompatibility. Mater Sci Eng B 2011;176:1600–8. doi:10.1016/j.mseb.2011.05.028

[12] Witte F. The history of biodegradable magnesium implants: A review. Acta Biomater 2010;6:1680–92. doi:10.1016/j.actbio.2010.02.028

[13] Wang J-L, Xu J-K, Hopkins C, Chow DH-K, Qin L. Biodegradable Magnesium-Based Implants in Orthopedics – A General Review and Perspectives. Adv Sci 2020;7:1902443. doi:10.1002/advs.201902443

[14] Rahman M, Dutta NK, Roy Choudhury N. Magnesium Alloys With Tunable Interfaces as Bone Implant Materials. Front Bioeng Biotechnol 2020;Volume 8-2020. doi:10.3389/fbioe.2020.00564

[15] Chandra G, Pandey A. Design approaches and challenges for biodegradable bone implants: a review. Expert Rev Med Devices 2021;18:629–47. doi:10.1080/17434440.2021.1935875

[16] Heimann RB. Magnesium alloys for biomedical application: Advanced corrosion control through surface coating. Surf Coatings Technol 2021;405:126521. doi:10.1016/j.surfcoat.2020.126521

[17] Jahr H, Li Y, Zhou J, Zadpoor AA, Schröder K-U. Additively Manufactured Absorbable Porous Metal Implants – Processing, Alloying and Corrosion Behavior. Front Mater 2021;Volume 8-2021. doi:10.3389/fmats.2021.628633

[18] Hornberger H, Virtanen S, Boccaccini AR. Biomedical coatings on magnesium alloys – A review. Acta Biomater 2012;8:2442–55. doi:10.1016/j.actbio.2012.04.012

[19] Wang J, Tang J, Zhang P, Li Y, Wang J, Lai Y, et al. Surface modification of magnesium alloys developed for bioabsorbable orthopedic implants: A general review. J Biomed Mater Res Part B Appl Biomater 2012;100B:1691–701. doi:10.1002/jbm.b.32707

[20] Yang J, Cui F, Lee IS. Surface Modifications of Magnesium Alloys for Biomedical Applications. Ann Biomed Eng 2011;39:1857–71. doi:10.1007/s10439-011-0300-y

[21] Huo H, Li Y, Wang F. Corrosion of AZ91D magnesium alloy with a chemical conversion coating and electroless nickel layer. Corros Sci 2004;46:1467–77. doi:10.1016/j.corsci.2003.09.023

[22] Xue D, Yun Y, Schulz MJ, Shanov V. Corrosion protection of biodegradable magnesium implants using anodization. Mater Sci Eng C 2011;31:215–23. doi:10.1016/j.msec.2010.08.019

[23] Jothi V, Adesina AY, Kumar AM, Rahman MM, Ram JSN. Enhancing the biodegradability and surface protective performance of AZ31 Mg alloy using polypyrrole/gelatin composite coatings with anodized Mg surface. Surf Coatings Technol 2020;381:125139. doi:10.1016/j.surfcoat.2019.125139

[24] Kocijan A, Kovač J, Junkar I, Resnik M, Kononenko V, Conradi M. The Influence of Plasma Treatment on the Corrosion and Biocompatibility of Magnesium. Materials (Basel) 2022;15. doi:10.3390/ma15207405

[25] Li C-Y, Feng X-L, Fan X-L, Yu X-T, Yin Z-Z, Kannan MB, et al. Corrosion and Wear Resistance of Micro-Arc Oxidation Composite Coatings on Magnesium Alloy AZ31—The Influence of Inclusions of Carbon Spheres. Adv Eng Mater 2019;21:1900446. doi:10.1002/adem.201900446

[26] Conradi M, Kocijan A, Podgornik B. Enhancing Magnesium Bioactivity for Biomedical Applications: Effects of Laser Texturing and Sandblasting on Surface Properties. Materials (Basel) 2024;17. doi:10.3390/ma17204978

[27] Park J, Park B-I, Son YJ, Lee SH, Um S-H, Kim Y-C, et al. Femtosecond laser-mediated anchoring of polymer layers on the surface of a biodegradable metal. J Magnes Alloy 2021;9:1373–81. doi:10.1016/j.jma.2020.12.003

[28] Fajardo S, Miguélez L, Arenas MA, de Damborenea J, Llorente I, Feliu S. Corrosion resistance of pulsed laser modified AZ31 Mg alloy surfaces. J Magnes Alloy 2022;10:756–68. doi:10.1016/j.jma.2021.09.020

[29] Stepanovska J, Matejka R, Rosina J, Bacakova L, Kolarova H. Treatments for enhancing the biocompatibility of titanium implants. Biomed Pap 2020;164:23–33. doi:10.5507/bp.2019.062

[30] Zhao L, Mei S, Chu PK, Zhang Y, Wu Z. The influence of hierarchical hybrid micro/nano-textured titanium surface with titania nanotubes on osteoblast functions. Biomaterials 2010;31:5072–82. doi:10.1016/J.BIOMATERIALS.2010.03.014

[31] Oliver WC, Pharr GM. Measurement of hardness and elastic modulus by instrumented indentation: Advances in understanding and refinements to methodology. J Mater Res 2004;19:3–20. doi:10.1557/jmr.2004.19.1.3

[32] K.R. R, Bontha S, M.R. R, Das M, Balla VK. Degradation, wettability and surface characteristics of laser surface modified Mg–Zn–Gd–Nd alloy. J Mater Sci Mater Med 2020;31:42. doi:10.1007/s10856-020-06383-9

[33] Pulido-González N, Torres B, Zheludkevich ML, Rams J. High Power Diode Laser (HPDL) surface treatments to improve the mechanical properties and the corrosion behaviour of Mg-Zn-Ca alloys for biodegradable implants. Surf Coatings Technol 2020;402:126314. doi:10.1016/J.SURFCOAT.2020.126314

[34] Iwaszko J, Strzelecka M. Effect of cw-CO2 laser surface treatment on structure and properties of AZ91 magnesium alloy. Opt Lasers Eng 2016;81:63–9. doi:10.1016/J.OPTLASENG.2016.01.009

[35] Wenzel RN. Resistance of solid surfaces to wetting by water. Ind Eng Chem, 1936;28